

# Decay of Scalar Condensation in Quantum Field Theory

Shigeki Matsumoto<sup>(a,b)</sup> and Takeo Moroi<sup>(a)</sup>

<sup>(a)</sup>*Department of Physics, Tohoku University, Sendai 980-8578, Japan*

<sup>(b)</sup>*Tohoku University International Advanced Research and Education Organization,  
Institute for International Advanced Interdisciplinary Research,  
Sendai 980-8578, Japan*

## Abstract

We consider decay processes of scalar-field condensation in the framework of well-established quantum field theory. We postulate that the quantum state corresponding to the scalar-field condensation is so-called coherent state with discussing the validity of such a treatment. We show that, by using the unitarity relation of the scattering matrix, decay rate of the coherent state is systematically calculated. We apply our procedure to derive explicit formulae of decay rates for two cases: (i) we study the case where the scalar condensation decays into a pair of scalar particles and show that our formalism reproduces the results obtained from the parametric-resonance analysis, and (ii) we also calculate the decay rate when the coherent state decays via anomaly.

# 1 Introduction

Scalar-field condensations play very crucial roles in various places in cosmology. Probably the most important example is the inflaton field which is necessary for inflation [1, 2]. In particular, in the slow-roll inflation models [3, 4], energy density of the inflaton condensation provides the energy density to realize (quasi-) de-Sitter universe during inflation. After inflation, the inflaton oscillates around the minimum of the potential and decays into standard-model particles to reheat the universe realizing hot big-bang cosmology. This class of inflation model not only solves flatness and horizon problems in cosmology but also provides density fluctuation consistent with the Wilkinson Microwave Anisotropy Probe data [5]. In addition, it has been pointed out that the density fluctuation may arise from late-decaying scalar field other than the inflaton, which is called “curvaton” [6, 7, 8]. Other important example is the Affleck-Dine field for baryogenesis [9]. In low-energy supersymmetric models, there exist scalar fields, i.e., scalar partners of quarks, which have baryon number. If some of those fields acquire non-vanishing amplitudes in the early universe, non-vanishing baryon number may be imprinted into the motion of the scalar-quark condensations due to baryon-number violating operators at an ultra-high energy scale. Such a scenario is one of the most attractive scenario to generate large enough baryon asymmetry of the universe.

All of these exotic scalar-field condensations (i.e, inflaton, curvaton, Affleck-Dine field, and so on) oscillate around the minimum of the potential at some stage of the evolution of the universe, and eventually decay into standard-model particles for the cosmological history consistent with observations. Thus, it is important to understand how the scalar-field condensation decays from the view point of the quantum field theory.

The main concern of this paper is to discuss how the oscillating scalar-field condensation decays into other states. Around the minimum, the potential of the scalar field  $\varphi$  is well estimated by a parabolic one

$$V = \frac{1}{2}m_\varphi^2\varphi^2. \quad (1.1)$$

Neglecting the effect of the cosmic expansion for simplicity, the solution to the classical equation of motion is given by

$$\varphi = A_\varphi \cos m_\varphi t. \quad (1.2)$$

In this case, the energy density of the condensation is given by  $\rho_\varphi = \frac{1}{2}m_\varphi^2 A_\varphi^2$ . One should understand how the energy density stored in the oscillation of  $\varphi$  is converted to the that of radiation. In the simplest approach, the decay rate of the scalar-field condensation is estimated from the decay rate of single scalar field (in the vacuum): the energy density of the scalar field in the condensation is approximated to decrease as

$$\frac{d\rho_\varphi}{dt} = -\gamma_\varphi\rho_\varphi, \quad (1.3)$$

where  $\gamma_\varphi$  is the decay rate of  $\varphi$  in the vacuum. However, it has been also pointed out that, when the scalar field  $\varphi$  is oscillating like Eq. (1.2), wave functions of fields which couple

to  $\varphi$  are modified. Consequently, the “decay rate” of the scalar field in the condensation may be significantly different from the one obtained from the field theory in the vacuum. In particular, in some of the cases, instability band may arise in the wave function of the final-state particles, which results in catastrophic particle production (so-called parametric resonance) [10, 11, 12, 13]. Since the decay of scalar-field condensation is very important, it is desirable to have a deep understanding of the decay processes of scalar-field oscillations in the framework of well-established quantum field theory.

In this paper, we consider decay processes of scalar condensations in the framework of the quantum field theory. In our analysis, we neglect the effects of cosmic expansion as a first step to understand the behavior of the scalar condensation. We postulate that the scalar condensation corresponds to the so-called coherent state  $|\varphi\rangle$  in the quantum field theory; justification of such a treatment will be also discussed. Then, we will show that the decay rate of the coherent state can be systematically calculated by using the unitarity relation of the scattering matrix ( $S$ -matrix). By using the fact that the decay rate of the coherent state is proportional to the imaginary part of the so-called  $T$ -matrix element  $\Im[\langle\varphi|\hat{T}|\varphi\rangle]$ , we formulate the calculation of the decay rate of the coherent state. We apply our procedure to the case where the scalar-field condensation is coupled to a real scalar field and calculate the decay rate for such a case. We will see that our procedure gives the same decay rate as that obtained by the discussion of parametric-resonance. We discuss when Eq. (1.3) is justified and how the instability band for parametric resonance arises in our framework. We also calculate the decay rate of scalar condensation which decays into gauge-boson pair via anomaly.

Organization of this paper is as follows. In Section 2, we first derive basic formulae which are used in the calculation of the decay rate of the coherent state. In particular, we define the coherent state  $|\varphi\rangle$  in the quantum field theory and present important properties of  $|\varphi\rangle$ . Then, we explain how the decay rate of the state  $|\varphi\rangle$  is obtained. In Section 3, we consider the case where the condensation couples to a real scalar field  $\chi$  via three-point interaction. Decay of the coherent state via the interaction induced by the anomaly is discussed in Section 4. In Section 5, we summarize our results.

## 2 Basic Formulae

In this section, we introduce basic formulae used in our analysis. We discuss how the condensation of scalar field decays via some interaction. We assume that the interaction of the scalar field is weak enough.

Total decay rate of any state can be related to the imaginary part of the scattering-matrix element due to the  $S$ -matrix unitarity. Let us denote the  $S$ -matrix as

$$\hat{S} = \hat{\mathbf{1}} + i\hat{T}, \quad (2.1)$$

where  $\hat{\mathbf{1}}$  and  $\hat{T}$  are the unit operator and the so-called  $T$ -matrix, respectively. (Here and hereafter, the “hat” is used for operators.) Then, from the unitarity of the  $S$ -matrix, the

following relation holds:

$$\hat{\mathcal{T}}^\dagger \hat{\mathcal{T}} = i(\hat{\mathcal{T}}^\dagger - \hat{\mathcal{T}}). \quad (2.2)$$

This relation is important for our analysis.

We expect that there exists a quantum state  $|\varphi\rangle$  which describes the state with scalar condensation. (Details about  $|\varphi\rangle$  will be explained below.) The probability of the state  $|\varphi\rangle$  decaying into all the possible final states is related to the imaginary part of the  $T$ -matrix element as

$$\text{Prob}(|\varphi\rangle \rightarrow \text{all}) = \sum_f \left| \langle f | \hat{\mathcal{T}} | \varphi \rangle \right|^2 = 2\Im \left[ \langle \varphi | \hat{\mathcal{T}} | \varphi \rangle \right]. \quad (2.3)$$

Now, we consider what the state  $|\varphi\rangle$  is. We first quantize the field operator using the free part of the Lagrangian, then treat the interaction terms as perturbations. We denote the free part of the Lagrangian of the real scalar field  $\varphi$  as

$$\mathcal{L} = \frac{1}{2} \partial_\mu \varphi \partial^\mu \varphi - \frac{1}{2} m_\varphi^2 \varphi^2. \quad (2.4)$$

In our analysis, we use the box normalization of the wave functions with the volume  $L^3$ . Then, the field operator is given by

$$\hat{\varphi}(x) = \sum_{\mathbf{k}} \frac{1}{\sqrt{2E_{\mathbf{k}}L^3}} \left( \hat{a}_{\mathbf{k}} e^{-ikx} + \hat{a}_{\mathbf{k}}^\dagger e^{ikx} \right), \quad (2.5)$$

where  $E_{\mathbf{k}} \equiv \sqrt{\mathbf{k}^2 + m_\varphi^2}$ . The annihilation and creation operators satisfy the following commutation relations:

$$[\hat{a}_{\mathbf{k}}, \hat{a}_{\mathbf{k}'}^\dagger] = \delta_{\mathbf{k}, \mathbf{k}'}, \quad (2.6)$$

while  $\hat{a}_{\mathbf{k}}$  and  $\hat{a}_{\mathbf{k}'}$  (as well as  $\hat{a}_{\mathbf{k}}^\dagger$  and  $\hat{a}_{\mathbf{k}'}^\dagger$ ) commute.

We postulate that the quantum state describing the scalar-field condensation is the coherent state, which is given by

$$|\varphi\rangle \equiv e^{-|C_\varphi|^2/2} e^{C_\varphi \hat{a}_0^\dagger} |0\rangle, \quad (2.7)$$

where  $|0\rangle$  is the vacuum state satisfying  $\hat{a}_{\mathbf{k}}|0\rangle = 0$ . Notice that the state  $|\varphi\rangle$  is properly normalized:  $\langle \varphi | \varphi \rangle = 1$ . In addition, importantly, the state  $|\varphi\rangle$  is an eigenstate of the annihilation operator  $\hat{a}_0$ :

$$\hat{a}_0 |\varphi\rangle = C_\varphi |\varphi\rangle. \quad (2.8)$$

We can also see that

$$\varphi(x) \equiv \langle \varphi | \hat{\varphi}(x) | \varphi \rangle = \varphi_-(x) + \varphi_+(x), \quad (2.9)$$

where

$$\varphi_-(x) \equiv \frac{1}{2}A_\varphi e^{-im_\varphi t}, \quad \varphi_+(x) \equiv \frac{1}{2}A_\varphi^* e^{im_\varphi t}, \quad (2.10)$$

with

$$A_\varphi = C_\varphi \sqrt{\frac{2}{m_\varphi L^3}}. \quad (2.11)$$

One can easily see that, for the coherent state  $|\varphi\rangle$ , the expectation value of the field operator follows the trajectory of the solution to the classical wave equation. Thus, we expect that the coherent state  $|\varphi\rangle$  corresponds to the quantum state where the scalar field is under oscillation.

In calculating  $T$ -matrix elements, it is necessary to calculate the expectation values of time-ordered products of field operators. By using the Wick's theorem, such products are calculated as

$$\begin{aligned} \langle \varphi | T \prod_i \hat{\varphi}(x_i) | \varphi \rangle &= \langle \varphi | N \prod_i \hat{\varphi}(x_i) | \varphi \rangle + (\text{all the possible contractions}) \\ &= \prod_i \varphi(x_i) + (\text{all the possible contractions}), \end{aligned} \quad (2.12)$$

where the symbol  $T$  here denotes the time-ordering while  $N$  is for normal-ordering. In addition, in the second equality, we have used Eq. (2.8). Even in more complicated cases, we obtain

$$\begin{aligned} \langle \varphi | T \prod_i f_i(\hat{\varphi}(x_i)) | \varphi \rangle &= \langle \varphi | T \prod_i \sum_n \frac{1}{n!} \left[ \frac{d^n f_i}{d\varphi^n} \right]_{\varphi(x_i)} (\hat{\varphi}(x_i) - \varphi(x_i))^n | \varphi \rangle \\ &= \prod_i f_i(\varphi(x_i)) + (\text{all the possible contractions}). \end{aligned} \quad (2.13)$$

Here, we expand  $f_i(\hat{\varphi}(x_i))$  around  $\hat{\varphi}(x_i) = \varphi(x_i)$ . Then,  $\langle \varphi | (\hat{\varphi}(x) - \varphi(x)) | \varphi \rangle = 0$ , and Eq. (2.13) is applicable even when the function  $f_i(\varphi)$  is singular at  $\varphi = 0$ .

In the following, we will not consider the processes in which  $\varphi$  is produced due to the decay of the coherent state. (The inclusion of such processes is straightforward.) In such a case, propagator of  $\varphi$  does not show up in the calculation and the field operator  $\hat{\varphi}(x)$  can be simply replaced by the expectation value  $\varphi(x)$ , in which the contraction terms are irrelevant.

It is also instructive to calculate the expectation values of energy-density operator as

$$\rho_\varphi = L^{-3} \langle \varphi | \sum_{\mathbf{k}} E_{\mathbf{k}} \hat{a}_{\mathbf{k}}^\dagger \hat{a}_{\mathbf{k}} | \varphi \rangle = \frac{1}{2} m_\varphi^2 |A_\varphi|^2, \quad (2.14)$$

while the expectation value of the number density is also given by

$$n_\varphi = L^{-3} \langle \varphi | \sum_{\mathbf{k}} \hat{a}_{\mathbf{k}}^\dagger \hat{a}_{\mathbf{k}} | \varphi \rangle = \frac{1}{2} m_\varphi |A_\varphi|^2. \quad (2.15)$$

For the complex scalar field (which we denote as  $\phi$ ), similar argument applies. We define the field operator for the complex scalar field as

$$\hat{\phi}(x) = \sum_{\mathbf{k}} \frac{1}{\sqrt{2E_{\mathbf{k}}L^3}} \left( \hat{a}_{\mathbf{k}} e^{-ikx} + \hat{b}_{\mathbf{k}}^{\dagger} e^{ikx} \right), \quad (2.16)$$

where  $\hat{a}_{\mathbf{k}}$  and  $\hat{b}_{\mathbf{k}}$  ( $\hat{a}_{\mathbf{p}}^{\dagger}$  and  $\hat{b}_{\mathbf{k}}^{\dagger}$ ) are annihilation (creation) operators. The coherent state for the complex field is given by

$$|\phi\rangle \equiv e^{-(|C_{\phi}|^2 + |C_{\bar{\phi}}|^2)/2} e^{C_{\phi}\hat{a}_0^{\dagger} + C_{\bar{\phi}}\hat{b}_0^{\dagger}} |0\rangle, \quad (2.17)$$

and

$$\phi(x) \equiv \langle \phi | \hat{\phi}(x) | \phi \rangle = A_{\phi} e^{-im_{\phi}t} + A_{\bar{\phi}}^* e^{im_{\phi}t}, \quad (2.18)$$

where

$$A_{\phi} = \frac{C_{\phi}}{\sqrt{2m_{\phi}L^3}}, \quad A_{\bar{\phi}} = \frac{C_{\bar{\phi}}}{\sqrt{2m_{\phi}L^3}}. \quad (2.19)$$

Energy density of this state is given by

$$\rho_{\phi} = 2m_{\phi}^2 (|A_{\phi}|^2 + |A_{\bar{\phi}}|^2), \quad (2.20)$$

while we can also calculate the expectation values of the number densities of particle  $\phi$  and anti-particle  $\bar{\phi}$  as

$$n_{\phi} \equiv L^{-3} \langle \phi | \sum_{\mathbf{k}} \hat{a}_{\mathbf{k}}^{\dagger} \hat{a}_{\mathbf{k}} | \phi \rangle = 2m_{\phi} |A_{\phi}|^2, \quad (2.21)$$

$$n_{\bar{\phi}} \equiv L^{-3} \langle \phi | \sum_{\mathbf{k}} \hat{b}_{\mathbf{k}}^{\dagger} \hat{b}_{\mathbf{k}} | \phi \rangle = 2m_{\phi} |A_{\bar{\phi}}|^2. \quad (2.22)$$

We can see that the number densities of  $\phi$  and its anti-particle are proportional to  $|A_{\phi}|^2$  and  $|A_{\bar{\phi}}|^2$ , respectively. Thus, when  $|A_{\phi}| > |A_{\bar{\phi}}|$  ( $|A_{\phi}| < |A_{\bar{\phi}}|$ ),  $\phi$  is more (less) abundant than  $\bar{\phi}$  in the condensation. It should be also noted that the function  $\phi(x)$  given in Eq. (2.18) gives an elliptical trajectory on the complex  $\phi$ -plane. When  $A_{\phi} = 0$  or  $A_{\bar{\phi}} = 0$ , the trajectory becomes a circle and, when  $|A_{\phi}| = |A_{\bar{\phi}}|$ , the trajectory becomes a straight line.

### 3 Decay into Scalar Fields

#### 3.1 Setup

First, we consider the simplest case where the scalar field  $\varphi$  couples only to the real scalar field  $\chi$  via the interaction

$$\mathcal{L}_{\text{int}} = -\frac{1}{2} \mu \varphi \chi^2, \quad (3.1)$$

with  $\mu$  being the coupling constant. With this interaction, the decay rate of single particle in the vacuum is given by

$$\gamma_{\varphi \rightarrow \chi\chi} = \frac{\mu^2}{32\pi m_\varphi} \sqrt{1 - \left(\frac{4m_\chi^2}{m_\varphi^2}\right)}. \quad (3.2)$$

In this section, with the interaction given in Eq. (3.1), we discuss how the coherent state decays.

As discussed in the previous section, the decay rate of the coherent state can be related to the imaginary part of the diagonal element of the  $T$ -matrix  $\langle \varphi | \hat{\mathcal{T}} | \varphi \rangle$ . Importantly,  $\langle \varphi | \hat{\mathcal{T}} | \varphi \rangle$  is obtained by calculating loop diagrams in the quantum field theory.

At the one-loop level, in other words, neglecting the fluctuation of  $\varphi$ ,  $\langle \varphi | \hat{\mathcal{T}} | \varphi \rangle$  is expressed as

$$\langle \varphi | \hat{\mathcal{T}} | \varphi \rangle \equiv \sum_{p=1}^{\infty} \sum_{\mathcal{F}^{(2p)}} \mathcal{T}^{\mathcal{F}^{(2p)}}, \quad (3.3)$$

where the summation over  $\mathcal{F}^{(2p)}$  is for all the possible Feynman diagrams with  $2p$  external  $\varphi$ . With  $p$  being fixed, one can find

$$\sum_{\mathcal{F}^{(2p)}} i\mathcal{T}^{\mathcal{F}^{(2p)}} = \frac{1}{(2p)!} \left(\frac{i\mu}{2}\right)^{2p} \langle 0 | T \left[ \int d^4x \{ \varphi_-(x) + \varphi_+(x) \} \hat{\chi}(x) \hat{\chi}(x) \right]^{2p} | 0 \rangle, \quad (3.4)$$

where  $\varphi_-$  and  $\varphi_+$  show up when the field operator  $\hat{\varphi}$  is contracted with the creation operator in  $|\varphi\rangle$  and the annihilation operator in  $\langle\varphi|$ , respectively. In order to obtain non-vanishing results, we need to pick up same number of  $\varphi_-$  and  $\varphi_+$ .

The right-hand side of Eq. (3.4) contains contribution from various Feynman diagrams because  $\varphi_-$  and  $\varphi_+$  can be ordered in many ways. In Fig. 1, we show a typical diagram (after imposing the cut). In our notation, we represent the insertion of  $\varphi_-$  by the white dot  $\circ$  while  $\varphi_+$  by the black dot  $\bullet$ ; non-vanishing diagrams have  $p$  black and  $p$  white dots. Internal lines are  $\chi$ -propagator.

Expectation value of  $\hat{\mathcal{T}}$  for the given diagram  $\mathcal{F}^{(2p)}$  (with  $2p$  external  $\varphi$  insertion) is given by

$$i\mathcal{T}^{\mathcal{F}^{(2p)}} = L^3 T S_{\mathcal{F}} \left| \frac{\mu A_\varphi}{2} \right|^{2p} \int \frac{d^4 \tilde{k}}{(2\pi)^4} \prod_{I=1}^{2p} (k_I^2 - m_\chi^2 + i0^+)^{-2}, \quad (3.5)$$

where  $S_{\mathcal{F}}$  is the symmetry factor and

$$L^3 T = \int d^4x. \quad (3.6)$$

In addition, the momentum flowing on the  $I$ -th propagator is given by

$$k_I \equiv \tilde{k} + \sum_{J=1}^I \varepsilon_J Q_\varphi, \quad (3.7)$$

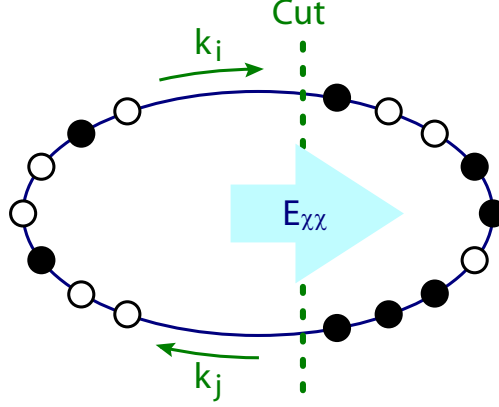


Figure 1: An example of the Feynman diagram which gives rise to the imaginary part of  $\langle \varphi | \hat{\mathcal{T}} | \varphi \rangle$ . The white dot  $\circ$  indicates  $\varphi_-$  insertion while the black dot  $\bullet$  is for  $\varphi_+$  insertion. In this example,  $p = 8$  and, with the cut shown in the figure,  $N_\varphi = 3$ . (Notice that other cuts are also possible with this diagram.)

with

$$Q_\varphi \equiv (m_\varphi, \mathbf{0}), \quad (3.8)$$

and  $\varepsilon_J = 1$  and  $-1$  if the  $J$ -th  $\varphi$  insertion is  $\varphi_-$  and  $\varphi_+$ , respectively.

The imaginary part of  $\mathcal{T}^{\mathcal{F}(2p)}$  is obtained by cutting two propagators (see Fig. 1), which corresponds to the replacements of those two propagators by the  $\delta$ -functions (with a relevant numerical factor):

$$\Im [\mathcal{T}^{\mathcal{F}(2p)}] = \lim_{\xi \rightarrow m_\chi^2} \sum_{i=1}^{2p-1} \sum_{j=i+1}^{2p} \Im [\mathcal{T}_{i,j}^{\mathcal{F}(2p)}(\xi)], \quad (3.9)$$

where

$$\Im [\mathcal{T}_{i,j}^{\mathcal{F}(2p)}(\xi)] \equiv 2\pi^2 L^3 T S_{\mathcal{F}} \left| \frac{\mu A_\varphi}{2} \right|^{2p} \int \frac{d^4 \tilde{k}}{(2\pi)^4} \delta(k_i^2 - \xi_i) \delta(k_j^2 - \xi_j) \prod_{I \neq i,j} (k_I^2 - \xi_I)^{-1}. \quad (3.10)$$

(For details, see Appendix A.)  $\Im [\mathcal{T}_{i,j}^{\mathcal{F}(2p)}]$  is the contribution from the diagram in which cut is on  $i$ - and  $j$ -th propagators. For  $\Im [\mathcal{T}_{i,j}^{\mathcal{F}(2p)}]$ , we define the energy flow from one side of the cut to the other, which we denote  $E_{\chi\chi}$ ; with the following non-negative integer:

$$N_\varphi = \left| \sum_{I=i+1}^j \varepsilon_I \right|, \quad (3.11)$$

the energy flow is given by

$$E_{\chi\chi} = N_\varphi m_\varphi. \quad (3.12)$$



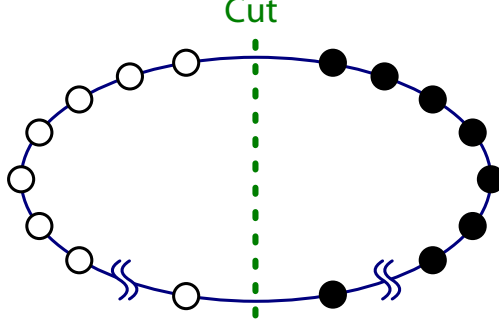


Figure 2: Feynman diagram which gives the leading-order contribution to the decay rate in the small amplitude limit. The white dot  $\circ$  indicates  $\varphi_-$  insertion while the black dot  $\bullet$  is for  $\varphi_+$  insertion.

Notice that  $\Im[\mathcal{T}_{i,j}^{\mathcal{F}(2p)}]$  contributes only to the decay rate of the process in which  $N_\varphi$  of  $\varphi$  in the condensation simultaneously annihilate into two  $\chi$  because we neglect the fluctuations of the  $\varphi$  field. At the perturbative level, such a decay process is kinematically allowed when  $E_{\chi\chi} > 2m_\chi$ .

### 3.2 Small amplitude limit

In this and the next subsections, we concentrate on the case where the amplitude of  $\varphi$  is small. In this case, the leading-order contribution to the  $E_\varphi = N_\varphi m_\phi$  mode is from the diagram with  $2N_\varphi$  external  $\varphi$  with  $\varphi_-$  and  $\varphi_+$  being completely separated by the cut. (See Fig. 2.) Concentrating on such a leading-order diagram, the imaginary part of the  $T$ -matrix element is given by

$$\begin{aligned} \Im[\mathcal{T}_{\text{Leading}}^{(N_\varphi)}] &= L^3 T \pi^2 \left| \frac{\mu A_\varphi}{2} \right|^{2N_\varphi} \int \frac{d^4 \tilde{k}}{(2\pi)^4} \delta(\tilde{k}^2 - m_\chi^2) \delta((\tilde{k} - N_\varphi Q_\varphi)^2 - m_\chi^2) \\ &\quad \prod_{I=1}^{N_\varphi-1} [(\tilde{k} - I Q_\varphi)^2 - m_\chi^2]^{-2}. \end{aligned} \quad (3.13)$$

Constraints from the  $\delta$ -functions give  $\tilde{k} Q_\varphi = \frac{1}{2} N_\varphi m_\varphi^2$ . Thus,

$$\prod_{I=1}^{N_\varphi-1} [(\tilde{k} - I Q_\varphi)^2 - m_\chi^2]^{-1} \rightarrow m_\varphi^{-4(N_\varphi-1)} [(N_\varphi - 1)!]^{-4}, \quad (3.14)$$

and hence

$$\Im[\mathcal{T}_{\text{Leading}}^{(N_\varphi)}] = L^3 T \frac{\beta_{N_\varphi}}{32\pi} \frac{m_\varphi^4}{[(N_\varphi - 1)!]^4} \left| \frac{\mu A_\varphi}{2m_\varphi^2} \right|^{2N_\varphi}, \quad (3.15)$$

where, for  $N_\varphi m_\varphi > 2m_\chi$ , the velocity  $\beta_{N_\varphi}$  is given by

$$\beta_{N_\varphi} \equiv \sqrt{1 - \frac{4m_\chi^4}{N_\varphi^2 m_\varphi^2}}, \quad (3.16)$$

while  $\beta_{N_\varphi} = 0$  for  $N_\varphi m_\varphi \leq 2m_\chi$ .

The decay rate of the coherent state  $|\varphi\rangle$  per unit volume is evaluated as

$$(\text{Decay rate per unit volume}) = \frac{\text{Prob}(|\varphi\rangle \rightarrow \text{all})}{L^3 T}, \quad (3.17)$$

and hence is given by

$$\Gamma_{\text{Leading}}^{(N_\varphi)} = \frac{\beta_{N_\varphi}}{16\pi} \frac{m_\varphi^4}{[(N_\varphi - 1)!]^4} \left| \frac{\mu A_\varphi}{2m_\varphi^2} \right|^{2N_\varphi}. \quad (3.18)$$

The above expression is consistent with the result given in the study of the parametric resonance [12]. In addition, the decay rate for the  $N_\varphi = 1$  mode is related to the decay rate of single particle, which is given in Eq. (3.2), as

$$\Gamma_{\text{Leading}}^{(N_\varphi=1)} = n_\varphi \gamma_{\varphi \rightarrow \chi\chi}. \quad (3.19)$$

Thus, when the amplitude of  $\varphi$  is small, decay of the coherent state can be treated as the decay of individual particles in the condensation, which justifies the conventional treatment of the decay processes of scalar condensations.

We also comment here that the decay rate given in Eq. (3.18) is also derived from the tree-level calculation of the  $\chi\chi$  pair creation rate in the external oscillating  $\varphi$  field;  $\Gamma_{\text{Leading}}^{(N_\varphi)}$  is equal to the production rate of  $\chi\chi$  pair per unit volume with total energy of  $E_{\chi\chi} = N_\varphi m_\varphi$ . In general, at the leading order of  $A_\varphi$ , the decay rate of the coherent state is also obtained by calculating the tree-level production rate of the final-state particles treating the scalar condensation as an external field. If we consider higher order contributions, however, such a calculation breaks down; treating the scalar condensation as the external field, denominators of some propagators vanish in certain types of diagrams. Notice that, in Eq. (3.9), such a difficulty does not exist. (See also the following discussion.)

### 3.3 Small velocity limit

In the previous subsection, we have calculated leading-order contributions to the decay rates of each mode in the small amplitude limit. Calculations of the contributions which are higher order in the amplitude are straightforward. In this subsection, we discuss when the small-amplitude expansion breaks down, taking the  $N_\varphi = 1$  mode as an example.

If we calculate  $O(|A_\varphi|^{2p})$  contributions to the decay rate of such mode, which are from diagrams with  $2p$  external  $\varphi$  insertions, one finds that the imaginary part of the  $T$ -matrix element is inversely proportional to the powers of  $\beta_1$  in the  $m_\varphi \rightarrow 2m_\chi$  limit. First, let us derive such a behavior with explicit calculation.

For the  $N_\varphi = 1$  mode, the most important Feynman diagrams in the  $m_\varphi \rightarrow 2m_\chi$  limit are those in which  $\varphi_+$  and  $\varphi_-$  insertions are next to each other. (See Fig. 3.) As we will discuss, other types of diagrams with fixed  $p$  have less singular behavior when  $\beta_1 \rightarrow 0$ . We also note

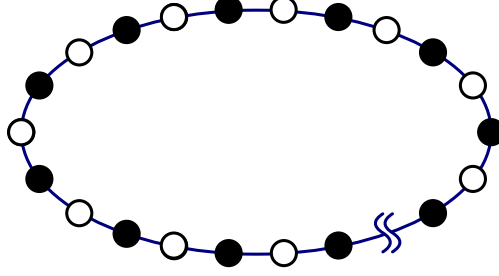


Figure 3: Feynman diagrams which give the most singular behavior for the  $N_\varphi = 1$  process in the small  $\beta_1$  limit. The white dot  $\circ$  indicates  $\varphi_-$  insertion while the black dot  $\bullet$  is for  $\varphi_+$  insertion.

here that the diagram in Fig. 3 contributes only to the  $N_\varphi = 1$  mode. (The imaginary part of the  $T$ -matrix vanishes when  $N_\varphi = 0$ .)

Taking into account the diagram shown in Fig. 3, the  $T$ -matrix element becomes

$$i\mathcal{T}_{\beta_1 \rightarrow 0}^{(N_\varphi=1)} = L^3 T \frac{1}{2p} \left| \frac{\mu A_\varphi}{2} \right|^{2p} \int \frac{d^4 \tilde{k}}{(2\pi)^4} (\tilde{k}^2 - m_\chi^2 + i0^+)^{-p} [(\tilde{k} - Q_\varphi)^2 - m_\chi^2 + i0^+]^{-p}, \quad (3.20)$$

and the imaginary part of  $\mathcal{T}_{\beta_1 \rightarrow 0}^{(N_\varphi=1)}$  is given by

$$\Im [\mathcal{T}_{\beta_1 \rightarrow 0}^{(N_\varphi=1)}] = -\frac{L^3 T}{32\pi} m_\varphi^4 \beta_1 \left| \frac{\mu A_\varphi}{2} \right|^2 \times \frac{(4p-7)!!}{p!(p-1)!} \left| \frac{\mu A_\varphi}{2m_\varphi^2 \beta_1^2} \right|^{2(p-1)} + O(\beta_1^{7-4p}), \quad (3.21)$$

where  $(2p-1)!! \equiv \prod_{I=1}^p (2I-1)$  for  $p \geq 1$ , and  $(-3)!! \equiv -1$ . (For details, see Appendix B.) Hereafter, we neglect  $O(\beta_1^{7-4p})$  contribution in Eq. (3.21), and the decay rate of the coherent state becomes

$$\Gamma_{\beta_1 \rightarrow 0}^{(N_\varphi=1)} = -\frac{1}{16\pi} m_\varphi^4 \beta_1 \left| \frac{\mu A_\varphi}{2} \right|^2 \sum_{p=1}^{\infty} \frac{(4p-7)!!}{p!(p-1)!} \left| \frac{\mu A_\varphi}{2m_\varphi^2 \beta_1^2} \right|^{2(p-1)}. \quad (3.22)$$

As discussed in Appendix B, the inverse powers of  $\beta_1$  stems from the derivative of the function  $B(m_\phi^2; \xi_i, \xi_j)$  given in Eq. (A.7) with respect to  $\xi_i$  or  $\xi_j$ . The order of the derivatives is equal to the number of the propagators whose denominators vanish in the on-shell limit  $\xi_i \rightarrow m_\chi^2$  ( $i = 1 - 2p$ ). Number of such propagators is maximized for the diagram given in Fig. 3. Thus, we safely neglect other types of diagrams in studying the case of  $\beta_1 \rightarrow 0$ .

As we mentioned,  $\Gamma_{\beta_1 \rightarrow 0}^{(N_\varphi=1)}$  becomes singular when  $\beta_1 \rightarrow 0$ . In other words, for the  $N_\varphi = 1$  mode, the small-amplitude expansion breaks down when  $|A_\varphi|$  is comparable to  $\mu^{-1} m_\varphi^2 \beta_1^2$ . These behaviors are related to the fact that instability bands appear in the solution to the classical wave equation of the scalar field (i.e.,  $\chi$  in our argument) which couples to a oscillating scalar field (i.e.,  $\varphi$ ). With the interaction given in Eq. (3.1), the wave equation of  $\chi$  (with the 3-momentum  $\mathbf{k}$ ) in the oscillating background is given by the Mathieu equation:

$$\frac{d^2 \chi_{\mathbf{k}}}{dt^2} + (\mathbf{k}^2 + m_\chi^2 + \mu |A_\varphi| \cos m_\varphi t) \chi_{\mathbf{k}} = 0. \quad (3.23)$$

Parametrizing the momentum of  $\chi$  as

$$\mathbf{k}^2 = \frac{1}{4}m_\varphi^2 (\beta_1^2 + \epsilon), \quad (3.24)$$

the lowest instability band in the small-amplitude limit is given by [12]

$$-\theta < \epsilon < \theta, \quad (3.25)$$

where

$$\theta \equiv \frac{2\mu|A_\varphi|}{m_\varphi^2}. \quad (3.26)$$

From the study of the parametric resonance, the momentum of  $\chi$  produced by the decay of the scalar condensation is in the range given by Eq. (3.25). For the consistency of the calculation, the mass of the initial-state particle  $\varphi$  should be large enough so that  $\mathbf{k}^2$  is positive even for  $\epsilon \sim -\theta$ ; otherwise,  $O(\theta^2)$  contributions may be also important. This argument gives the limitation of the small-amplitude approximation;  $\beta_1 \gg \theta^{1/2}$  is required, which results in  $|A_\varphi| \gg \mu^{-1}m_\varphi^2\beta_1^2$ .

The above argument is supported by the fact that  $\Gamma_{\beta_1 \rightarrow 0}^{(N_\varphi=1)}$  given in Eq. (3.22) is equal to the decay rate obtained by the parametric-resonance analysis. Indeed,  $\Gamma_{\beta_1 \rightarrow 0}^{(N_\varphi=1)}$  is also expressed as

$$\begin{aligned} \Gamma_{\beta_1 \rightarrow 0}^{(N_\varphi=1)} &= \frac{1}{2}m_\varphi \int_{|\mathbf{k}|_- < |\mathbf{k}| < |\mathbf{k}|_+} \frac{d^3\mathbf{k}}{(2\pi)^3} \lambda^{(N_\varphi=1)}(\mathbf{k}) \\ &= \frac{1}{128\pi^2} m_\varphi^4 \int_{-\theta}^{\theta} d\epsilon \sqrt{(\beta_1^2 + \epsilon)(\theta^2 - \epsilon^2)}, \end{aligned} \quad (3.27)$$

where, in the first equality,  $|\mathbf{k}|_\pm \equiv \frac{1}{2}m_\varphi\sqrt{\beta_1^2 \pm \theta}$ , and  $\lambda^{(N_\varphi=1)} = \frac{1}{2}\sqrt{\theta^2 - \epsilon^2}$  is the “growth-rate factor” for the  $N_\varphi = 1$  mode obtained in the study of the Mathieu equation [12]. The equivalence of Eq. (3.22) and Eq. (3.27) can be seen by expanding  $\sqrt{\beta_1^2 + \epsilon}$  in the integrand of Eq. (3.27) around  $\epsilon = 0$  (assuming  $\beta_1 > \theta^{1/2}$ ). Eq. (3.27) is nothing but the decay rate of the scalar condensation in the small-amplitude limit derived from the parametric-resonance analysis.

Eq. (3.27) (and Eq. (3.18)) also shows the fact that, at least at the small-amplitude limit, the results from the parametric-resonance analysis is obtained in our procedure where the quantum state describing the scalar condensation is postulated to be the coherent state. The equivalence of two approaches is also expected from the fact that the basic equations governing the behavior of the parametric resonance is derived in our framework. In particular, we can calculate the density matrix of the final-state particle  $\chi$  in the quantum field theory. We can see that the Mathieu equation shows up in the calculation and that the resultant density matrix is the same as the one obtained in the study of parametric resonance. These subjects will be discussed in the next subsection.

### 3.4 Calculation of the density matrix

In the classical treatment of the parametric resonant system, it is well known that the Mathieu equation appears as the equation of motion for the  $\chi$  field. Thus, the equation is also expected to be obtained in the quantum-field-theory treatment. In this subsection, we show the derivations of the Mathieu equation and the density matrix of  $\chi$  explicitly.

Since we are interested in the case where the scalar field  $\varphi$  initially forms the scalar condensation oscillating around the minimum of its potential, we describe the initial state (which is taken at  $t = 0$  in this subsection) as

$$|i\rangle = |\varphi\rangle \otimes |0\rangle_\chi, \quad (3.28)$$

where the first and second kets represent the states for  $\varphi$  and  $\chi$ , respectively. In addition,  $|0\rangle_\chi$  is the vacuum of the  $\chi$  field. (In the following, we omit the subscript  $\chi$ .)

For our argument, it is convenient to use the density matrix of the total system in the Schroedinger picture. The density matrix at the time  $T$  is simply given by

$$\hat{\rho}_{\text{tot}}(T) = e^{-i\hat{H}T} |i\rangle \langle i| e^{i\hat{H}T}, \quad (3.29)$$

with  $\hat{H}$  being the Hamiltonian of the total system. We consider the properties of  $\hat{\rho}_{\text{tot}}$  in the coordinate basis:

$$|q \otimes X\rangle \equiv |q\rangle \otimes |X\rangle, \quad (3.30)$$

where  $|q\rangle$  and  $|X\rangle$  are eigenstates of the field operators  $\hat{\varphi}$  and  $\hat{\chi}$ , respectively:

$$\hat{\varphi}(t, \mathbf{x})|q\rangle = q(\mathbf{x})|q\rangle, \quad \hat{\chi}(t, \mathbf{x})|X\rangle = X(\mathbf{x})|X\rangle. \quad (3.31)$$

Then, the density matrix in the coordinate basis,  $\rho_{\text{tot}}[q, X; q', X'] \equiv \langle q \otimes X | \hat{\rho}_{\text{tot}}(T) | q' \otimes X' \rangle$ , is given by

$$\begin{aligned} \rho_{\text{tot}}[q, X; q', X'] &= \int \mathcal{D}q_i \int \mathcal{D}q'_i \int \mathcal{D}X_i \int \mathcal{D}X'_i \langle q_i | \varphi \rangle \langle X_i | 0 \rangle \langle \varphi | q'_i \rangle \langle 0 | X'_i \rangle \\ &\quad K[q, X; q_i, X_i] K^*[q', X'; q'_i, X'_i]. \end{aligned} \quad (3.32)$$

The kernel is represented in the path integral form as

$$K[q, X; q_i, X_i] = \int_{\chi(0, \mathbf{x})=X_i(\mathbf{x})}^{\chi(T, \mathbf{x})=X(\mathbf{x})} \mathcal{D}\chi \int_{\varphi(0, \mathbf{x})=q_i(\mathbf{x})}^{\varphi(T, \mathbf{x})=q(\mathbf{x})} \mathcal{D}\varphi e^{iS_{\text{tot}}}, \quad (3.33)$$

where  $S_{\text{tot}}$  is the total action. For the explicit form of the kernel, see [14, 15].

In order to study the behavior of the  $\chi$  field, we derive the reduced density matrix of  $\chi$  by tracing out  $q$  and  $q'$  variables:

$$\rho_{\text{red}}[X; X'] \equiv \int \mathcal{D}q \rho_{\text{tot}}[q, X; q, X']. \quad (3.34)$$

For this purpose, we define

$$\tilde{q}_{\mathbf{k}} \equiv L^{-3/2} \int d^3\mathbf{x} q(\mathbf{x}) e^{-i\mathbf{k}\mathbf{x}}, \quad (3.35)$$

$$\tilde{X}_{\mathbf{k}} \equiv L^{-3/2} \int d^3\mathbf{x} X(\mathbf{x}) e^{-i\mathbf{k}\mathbf{x}}. \quad (3.36)$$

Then, with the use of the properties of the coherent state, we obtain the following relations:

$$\langle q|\varphi\rangle = \exp\left[-\frac{1}{2}m_\varphi(\tilde{q}_0 - L^{3/2}A_\varphi)^2\right] \prod_{\mathbf{k}\neq 0} \exp\left[-\frac{1}{2}E_{\mathbf{k}}|\tilde{q}_{\mathbf{k}}|^2\right], \quad (3.37)$$

$$\langle X|0\rangle = \prod_{\mathbf{k}} \exp\left[-\frac{1}{2}\omega_{\mathbf{k}}|\tilde{X}_{\mathbf{k}}|^2\right], \quad (3.38)$$

where, in this subsection, we consider the case where  $A_\varphi$  is real. ( $A_\varphi$  can be taken to be real with a relevant shift of the time variable.) In addition,  $\omega_{\mathbf{k}}^2 = \mathbf{k}^2 + m_\chi^2$ . In Eqs. (3.37) and (3.38), we omit unimportant numerical constants. Using Eq. (3.37), the reduced density matrix becomes

$$\rho_{\text{red}}[X; X'] = \int \mathcal{D}X_i \mathcal{D}X'_i \langle X_i|0\rangle \langle 0|X'_i\rangle \int_{\chi(0,\mathbf{x})=X_i}^{\chi(T,\mathbf{x})=X} \mathcal{D}\chi \int_{\chi'(0,\mathbf{x})=X'_i}^{\chi'(T,\mathbf{x})=X'} \mathcal{D}\chi' e^{i\bar{S}[\chi] - i\bar{S}[\chi'] + \mathcal{C}[\chi, \chi']}, \quad (3.39)$$

where

$$\bar{S}[\chi] = \int_0^T dt \int d^3\mathbf{x} \left[ \frac{1}{2} \partial_\mu \chi \partial^\mu \chi - \frac{1}{2} m_\chi^2 \chi^2 - \frac{1}{2} \mu A_\varphi \chi^2 \cos m_\varphi t \right], \quad (3.40)$$

while  $\mathcal{C}$  gives the collision terms:

$$\begin{aligned} \mathcal{C}[\chi, \chi'] &= -\frac{\mu^2}{4} \int_0^T dt \int_0^t dt' \int d^3\mathbf{x} \int d^3\mathbf{x}' \int \frac{d^3\mathbf{k}}{(2\pi)^3 2E_{\mathbf{k}}} \cos \mathbf{k}(\mathbf{x} - \mathbf{x}') \\ &\quad \left[ \chi^2(x) - \chi'^2(x) \right] \left[ e^{-iE_{\mathbf{k}}(t-t')} \chi^2(x') - e^{iE_{\mathbf{k}}(t-t')} \chi'^2(x') \right]. \end{aligned} \quad (3.41)$$

It can be seen that the periodic perturbation term,  $\chi^2 \cos m_\varphi t$ , appears in the reduced density matrix. Collision terms, which are proportional to  $\chi^4$ ,  $\chi'^4$ , and  $\chi^2 \chi'^2$ , also appear after the integration. Since no approximation was made to derive the density matrix, the above formula can be used at any amplitude of the  $\varphi$  field,  $A_\varphi$ . Furthermore, we can derive the kinetic equation by calculating the correlation function of the  $\chi$  field on the reduced density matrix, which allows us to describe the non-linear dynamics of the  $\chi$  system, as pointed out in [16].

When the amplitude  $A_\varphi$  is small enough, we can treat the collision terms as perturbations. Then, the reduced density matrix is, at the leading order calculation, written by using the wave functional of the  $\chi$  field:

$$\rho_{\text{red}}[X; X'] = \Psi[T, X] \times \Psi^*[T; X'], \quad (3.42)$$

where

$$\Psi[T, X] = \int \mathcal{D}X_i \langle X_i | 0 \rangle \int_{\chi(0, \mathbf{x})=X_i}^{\chi(T, \mathbf{x})=X} \mathcal{D}\chi e^{i\bar{S}[\chi]}. \quad (3.43)$$

The wave functional is written as a product of an infinite set of wave functions of harmonic oscillators as

$$\Psi[T, X] = \prod_{\mathbf{k}} \int_{-\infty}^{\infty} d\tilde{X}_{i, \mathbf{k}} \exp \left[ -\frac{1}{2} \omega_{\mathbf{k}} |\tilde{X}_{i, \mathbf{k}}|^2 \right] \int_{\tilde{\chi}_{\mathbf{k}}(0)=\tilde{X}_{i, \mathbf{k}}}^{\tilde{\chi}_{\mathbf{k}}(T)=\tilde{X}_{\mathbf{k}}} \mathcal{D}\tilde{\chi}_{\mathbf{k}} e^{i\bar{S}_{\mathbf{k}}[\tilde{\chi}_{\mathbf{k}}]}, \quad (3.44)$$

where

$$\bar{S}_{\mathbf{k}}[\tilde{\chi}_{\mathbf{k}}] = \int_0^T dt \left[ \frac{1}{2} |\dot{\tilde{\chi}}_{\mathbf{k}}|^2 - \frac{1}{2} (\mathbf{k}^2 + m_{\chi}^2 + \mu A_{\varphi} \cos m_{\varphi} t) |\tilde{\chi}_{\mathbf{k}}|^2 \right], \quad (3.45)$$

with the “dot” being the derivative with respect to time.  $\Psi[T, X]$  satisfies the boundary condition  $\Psi[0, X] = \prod_{\mathbf{k}} e^{-\omega_{\mathbf{k}} |\tilde{X}_{\mathbf{k}}|^2/2}$  (up to normalization), and its evolution is governed by the wave equation derived from the action given in Eq. (3.45). Thus,  $\Psi[T, X]$  is nothing but the wave functional obtained in [12]:

$$\Psi[T, X] = \prod_{\mathbf{k}} \frac{1}{\sqrt{u_{\mathbf{k}}(T)}} \exp \left[ \frac{i}{2} \frac{\dot{u}_{\mathbf{k}}(T)}{u_{\mathbf{k}}(T)} |\tilde{X}_{\mathbf{k}}|^2 \right], \quad (3.46)$$

where  $u_{\mathbf{k}}(t)$  is the solution to the Mathieu equation:

$$\frac{d^2 u_{\mathbf{k}}}{dt^2} + (\omega_{\mathbf{k}}^2 + \mu A_{\varphi} \cos m_{\varphi} t) u_{\mathbf{k}} = 0, \quad (3.47)$$

with the conditions  $u_{\mathbf{k}}(0) = \sqrt{\pi/\omega_{\mathbf{k}}}$  and  $\dot{u}_{\mathbf{k}}(0) = i\sqrt{\omega_{\mathbf{k}}\pi}$ . This fact supports that the scalar condensation is well described by the coherent state in the quantum field theory.

Before closing this section, we emphasize that the quantity  $\Im[\langle \varphi | \mathcal{T} | \varphi \rangle]$  is relatively easily calculated with wide variety of interactions and final-states. Thus, for some applications, our procedure is more powerful than the approach using the Mathieu equation.

## 4 Decay via Anomaly

Next, let us consider the case where a complex scalar field  $\phi$  may decay via chiral and conformal anomalies. As the fundamental theory, we expect that there exists chiral fermions which have gauge quantum numbers and that the complex scalar field couples to the chiral fermions through a Yukawa interaction. To make our discussion definite, we consider  $SU(N_c)$  gauge interaction; chiral fermions  $Q_L$  and  $Q_R^c$  are in fundamental and anti-fundamental representations of  $SU(N_c)$ , respectively, while  $\phi$  is singlet.

The complex scalar field couples to chiral fermions  $Q_L$  and  $Q_R^c$  via the Yukawa interaction

$$\mathcal{L}_{\text{Yukawa}} = -y(\phi Q_L Q_R^c + \text{h.c.}). \quad (4.1)$$

It should be noted that, in this model, there exists anomalous  $U(1)$  symmetry, which we call  $U(1)_A$ ; charges of  $\phi$ ,  $Q_L$  and  $Q_R^c$  are 1,  $-\frac{1}{2}$ , and  $-\frac{1}{2}$ , respectively.

When the amplitude of  $\phi$  is large, fermions  $Q_L$  and  $Q_R^c$  acquire Dirac mass. Thus, when  $m_\phi \ll y|\phi|$ , effective mass of the fermions are much larger than the mass of  $\phi$ . In this case, the decay process  $\phi \rightarrow Q_L Q_R^c$  is expected to be kinematically forbidden.

When  $m_\phi \ll y|\phi|$ , it is rather convenient to consider the low-energy effective field theory by integrating out the fermions. The relevant (light) fields in the low-energy effective field theory are  $\phi$  and gauge fields as far as the effective mass of the fermions are much larger than  $m_\phi$ . In the following, we concentrate on such a case; thus, we assume that the inequality  $m_\phi \ll y|\phi(x)|$  always holds at any point of the trajectory of  $\phi$ .

We first consider the effects of the operator induced by the chiral anomaly:

$$\mathcal{L}_{\text{eff}} = -i\lambda_I (\ln \phi - \ln \phi^\dagger) F^{\mu\nu} \tilde{F}_{\mu\nu}, \quad (4.2)$$

where  $F_{\mu\nu}$  is the field-strength tensor and

$$\tilde{F}^{\mu\nu} \equiv \frac{1}{2} \epsilon^{\mu\nu\rho\sigma} F_{\rho\sigma}. \quad (4.3)$$

In Eq. (4.2) and hereafter, summation over the adjoint gauge index is implicit. In addition,

$$\lambda_I \equiv \frac{g^2}{32\pi^2} T_R, \quad (4.4)$$

with  $g$  being the gauge coupling constant of  $SU(N_c)$ , and  $T_R = \frac{1}{2}$ .

Now, let us discuss the decay of the coherent state given in Eq. (2.17). At the leading order in  $\lambda_I$ , which is of  $O(\lambda_I^2)$  in the calculation of  $\langle \phi | \hat{\mathcal{T}} | \phi \rangle$ , we obtain

$$\begin{aligned} \langle \phi | i\hat{\mathcal{T}} | \phi \rangle &= -\frac{1}{2} \lambda_I^2 \int d^4x d^4x' \langle 0 | T \hat{F}_{\mu\nu}(x) \hat{\tilde{F}}^{\mu\nu}(x) \hat{F}_{\mu'\nu'}(x') \hat{\tilde{F}}^{\mu'\nu'}(x') | 0 \rangle \\ &\quad [\ln \phi(x) - \ln \phi^\dagger(x)] [\ln \phi(x') - \ln \phi^\dagger(x')]. \end{aligned} \quad (4.5)$$

In the following, we consider the case that  $A_\phi \geq A_{\bar{\phi}}$ . Then, we expand  $\ln \phi(x)$  as

$$\ln \phi(x) = \ln(A_\phi e^{-iQ_\phi x}) + \sum_{n=1}^{\infty} \frac{(-1)^{n-1}}{n} \left( \frac{A_{\bar{\phi}}^*}{A_\phi} \right)^n e^{2niQ_\phi x}, \quad (4.6)$$

where  $Q_\phi = (m_\phi, \mathbf{0})$ . At the lowest order in  $\lambda_I$ , the decay rate of the coherent state can be obtained by calculating the two-point functions of several types of operators with relevant momentum injection. For the local operator  $\hat{\mathcal{O}}(x)$ , let us define

$$\mathcal{I}_{\mathcal{O}}(Q) \equiv -i \int d^4x_1 d^4x_2 \langle 0 | T \hat{\mathcal{O}}(x_1) \hat{\mathcal{O}}(x_2) | 0 \rangle e^{iQ(x_1 - x_2)}. \quad (4.7)$$

Then, by using the fact that  $F_{\mu\nu} \tilde{F}^{\mu\nu}$  is expressed as a total derivative:

$$F_{\mu\nu} \tilde{F}^{\mu\nu} = \partial_\mu K^\mu = \frac{1}{2} \partial_\mu [\epsilon^{\mu\nu\rho\sigma} A_\nu (\partial_\rho A_\sigma) + (\text{gauge field})^3], \quad (4.8)$$



Eq. (4.5) becomes

$$\langle \phi | \hat{\mathcal{T}} | \phi \rangle = -2\lambda_I^2 \mathcal{I}_{Q_\phi^\mu K_\mu}(0) - \lambda_I^2 \sum_{n=1}^{\infty} \frac{1}{n^2} \left| \frac{A_{\bar{\phi}}}{A_\phi} \right|^{2n} \mathcal{I}_{F_{\mu\nu} \tilde{F}^{\mu\nu}}(2nQ_\phi). \quad (4.9)$$

It is notable that  $\mathcal{I}_{Q_\phi^\mu K_\mu}(0)$  has no imaginary part because there is no momentum injection into the internal gauge-boson lines from the  $Q_\phi^\mu K_\mu$ -vertex. Thus, the coherent state does not decay if  $A_\phi = 0$  or  $A_{\bar{\phi}} = 0$ . (This statement holds even after taking into account the higher order terms in  $\lambda_I$ .) This fact can be understood by the conservation of the  $U(1)_A$  charge. With a fixed value of the total energy of the system,  $U(1)_A$  charge is maximized when  $A_\phi = 0$  or  $A_{\bar{\phi}} = 0$ . Thus, if  $U(1)_A$  charge is conserved, the decay of  $\phi$  in the condensation into the gauge bosons is forbidden. Of course, the interaction given in Eq. (4.2) breaks  $U(1)_A$  symmetry because  $\mathcal{L}_{\text{eff}}$  is not invariant under the  $U(1)_A$  transformation. This is due to the fact that  $\mathcal{L}_{\text{eff}}$  is induced by the chiral anomaly. However, we can add new fermions, which we call  $Q'_L$  and  $Q'^c_R$ , to have conserved  $U(1)$  symmetry. Indeed, with  $Q'_L$  and  $Q'^c_R$ , which are in fundamental and anti-fundamental representation of  $SU(N_c)$ , respectively, we can define non-anomalous  $U(1)_A$  symmetry by assigning charge  $+\frac{1}{2}$  to both of  $Q'_L$  and  $Q'^c_R$ . (Notice that  $Q'_L$  and  $Q'^c_R$  do not have to couple to  $\phi$ .) In this case, conservation of the  $U(1)_A$  charge is obvious and the decay of  $\phi$  into the gauge bosons is completely forbidden. Thus, the  $U(1)_A$  charge stored in the scalar condensation cannot be released by the interaction given in Eq. (4.2). This fact may have some relevance in the study of the decay of scalar condensations in various cosmological scenarios, in particular, in the Affleck-Dine scenario [9]. In the absence of  $Q'_L$  and  $Q'^c_R$ , instanton effects may generate new interactions which explicitly breaks  $U(1)_A$  symmetry. In such a case, decay of the coherent state occurs via such new interactions.

Using the relation

$$\Im [\mathcal{I}_{F_{\mu\nu} \tilde{F}^{\mu\nu}}(Q)] = -\frac{N_c^2 - 1}{4\pi} (Q^2)^2 L^3 T, \quad (4.10)$$

the decay rate is given by

$$\Gamma_{F\tilde{F}} = \frac{\text{Prob}(|\phi\rangle \rightarrow \text{all})}{L^3 T} = \frac{8}{\pi} (N_c^2 - 1) \lambda_I^2 m_\phi^4 \sum_{n=1}^{\infty} n^2 \left| \frac{A_{\bar{\phi}}}{A_\phi} \right|^{2n}. \quad (4.11)$$

Since the decay rate vanishes if  $A_\phi = 0$  or  $A_{\bar{\phi}} = 0$ , the decay of the coherent state in this case should be understood as an annihilation between  $\phi$  and  $\bar{\phi}$  in the condensation; same number of  $\phi$  and  $\bar{\phi}$  annihilate into the gauge boson pair.

In the study of the decay of coherent state, the energy-loss rate is also important. Using the fact that the imaginary part of  $\mathcal{I}_{F_{\mu\nu} \tilde{F}^{\mu\nu}}(2nQ_\phi)$  is from the decay process into two gauge bosons with the total energy of  $2nm_\phi$ , the energy-loss rate can be calculated. So far, we have considered the case where  $A_\phi \geq A_{\bar{\phi}}$ . However, the decay rate for the case of  $A_\phi \leq A_{\bar{\phi}}$  is derived by interchanging  $A_\phi \leftrightarrow A_{\bar{\phi}}$  in the result. Thus, we obtain

$$\left[ \frac{d\rho_\phi}{dt} \right]_{F\tilde{F}} = -\frac{16}{\pi} (N_c^2 - 1) \lambda_I^2 m_\phi^5 \sum_{n=1}^{\infty} n^3 \left[ \frac{\min(n_\phi, n_{\bar{\phi}})}{\max(n_\phi, n_{\bar{\phi}})} \right]^n, \quad (4.12)$$

where we have used the fact that the number densities of  $\phi$  and  $\bar{\phi}$  are proportional to  $|A_\phi|^2$  and  $|A_{\bar{\phi}}|^2$ , respectively. (See Eqs. (2.21) and (2.22).) One may simplify the above energy-loss rate by using

$$\sum_{n=1}^{\infty} n^3 r^n = \frac{r(1+4r+r^2)}{(1-r)^4}. \quad (4.13)$$

Here, we emphasize that the results given in Eqs. (4.11) and (4.12) can be used for any value of the amplitude (as far as the effective mass of  $Q_L$  and  $Q_R^c$  are much larger than  $m_\phi$ ). When  $n_\phi \gg n_{\bar{\phi}}$  or  $n_\phi \ll n_{\bar{\phi}}$ , which corresponds to the case where the classical motion of the scalar condensation is almost circular, the energy-loss rate is well approximated by the leading term in Eq. (4.12). On the contrary, in the limit of  $n_{\bar{\phi}} \rightarrow n_\phi$ , higher order terms become important and the energy-loss rate is enhanced. In this case, however, one should note that, at some point of the classical trajectory,  $|\phi|$  approaches to the origin. Then, the effective mass of the fermions  $Q_L$  and  $Q_R^c$  may become so small that the effective field theory, which is obtained by integrating out these fermions, may break down. We also note that, with the ratio  $n_\phi/n_{\bar{\phi}}$  being fixed, the decay and energy-loss rates are independent of the amplitude of the scalar condensation.

Before closing this section, we also present the result for the case where the scalar field  $\phi$  couples to the gauge field as

$$\mathcal{L}_{\text{eff}} = \lambda_R (\ln \phi + \ln \phi^\dagger) F^{\mu\nu} F_{\mu\nu}. \quad (4.14)$$

This type of interaction is also generated by integrating out particles which acquire masses from the condensation of  $\phi$  (like  $Q_L$  and  $Q_R^c$ ). At the leading order in  $\lambda_R$ , the energy-loss rate is given by

$$\left[ \frac{d\rho_\phi}{dt} \right]_{FF} = -\frac{16}{\pi} (N_c^2 - 1) \lambda_R^2 m_\phi^5 \sum_{n=1}^{\infty} n^3 \left[ \frac{\min(n_\phi, n_{\bar{\phi}})}{\max(n_\phi, n_{\bar{\phi}})} \right]^n. \quad (4.15)$$

## 5 Summary

In this paper, we have discussed the decay processes of the scalar condensation. We postulated that the quantum state corresponding to the scalar oscillation is the so-called coherent state in the quantum field theory. Then, by using the  $S$ -matrix unitarity, we have developed the method to calculate the decay rate of the coherent state. We believe that our procedure can be applied to a large class of models which may contain various types of interactions.

Then, in order to demonstrate how the decay rate is calculated, we considered two examples. First, we studied the case where the scalar field  $\varphi$  couples to another scalar field  $\chi$  via three-point interaction. Using the small-amplitude approximation, we have calculated the decay rate for the process where  $N_\varphi$  ( $N_\varphi = 1, 2, 3, \dots$ ) of  $\varphi$  in the condensation simultaneously annihilate into a pair of  $\chi$ . For the case of  $N_\varphi = 1$ , we have seen that the result is the same as that in the conventional approach where the decay rate of the scalar condensation

is estimated by the product of the decay rate of single  $\varphi$  in the vacuum and the number density of  $\varphi$ . We have also pointed out that the small-amplitude approximation breaks down when the amplitude becomes close to  $\mu^{-1}m_\varphi^2\beta_1^2$ , where  $\mu$  is the coupling constant and  $\beta_1$  is the velocity of  $\chi$  in the  $N_\varphi = 1$  mode. Such a behavior is also expected from the discussion based on the parametric-resonance. Indeed, our procedure reproduced the decay rate of the scalar condensation calculated from the parametric-resonance analysis.

The second example was the case where the complex scalar field decays into gauge bosons via the interaction induced by the chiral anomaly. We have considered the case where the scalar potential has  $U(1)_A$  symmetry to rotate  $\phi \rightarrow e^{i\alpha}\phi$  at the classical level, which is broken by the effect of the chiral anomaly. In this case, we could calculate the decay rate without using the small-amplitude approximation. We have seen that the decay process is forbidden unless both the particle  $\phi$  and its anti-particle  $\bar{\phi}$  exist in the condensation, and that the “decay” of the coherent state is due to the annihilation between them. Thus,  $U(1)_A$  charge stored in the condensation cannot be released by the effective interaction induced by the chiral anomaly.

In our analysis, the effects of the cosmic expansion were completely neglected. However, we believe that our results are applicable to the cosmological discussion as far as the expansion rate of the universe is smaller than the mass of the scalar condensation.

*Acknowledgement:* This work was supported in part by the Grant-in-Aid for Scientific Research from the Ministry of Education, Science, Sports, and Culture of Japan, No. 19540255 (T.M.).

## A Calculation of the Imaginary Part

Although the technique which will be explained here is well-known, in this appendix, we show how Eq. (3.9) is derived for the sake of some of the readers. For this purpose, we calculate the imaginary part of the following quantity:

$$I_{\mathcal{F}}(Q_\varphi) \equiv -i \int \frac{d^4\tilde{k}}{(2\pi)^4} \prod_{I=1}^{2p} (k_I^2 - m_\chi^2 + i0^+)^2. \quad (\text{A.1})$$

Here,

$$k_I \equiv \tilde{k} + \sum_{J=1}^I \varepsilon_J Q_\varphi, \quad (\text{A.2})$$

where  $\varepsilon_I = \pm 1$  (with  $\varepsilon_1 + \cdots + \varepsilon_{2p} = 0$ ), and  $Q_\varphi = (m_\varphi, \mathbf{0})$ .

In order to calculate the imaginary part of  $I_{\mathcal{F}}$ , it is convenient to rewrite  $I_{\mathcal{F}}$  as

$$I_{\mathcal{F}} = -i \lim_{\xi \rightarrow m_\chi^2} \int \frac{d^4\tilde{k}}{(2\pi)^4} \prod_{I=1}^{2p} (k_I^2 - \xi + i0^+)^{-1}, \quad (\text{A.3})$$

where the limit  $\xi \rightarrow m_\chi^2$  indicates that  $\xi_I \rightarrow m_\chi^2$  ( $I = 1 - 2p$ ); before taking the limit,  $\xi_I$  are all set to be different. Integrand of Eq. (A.3) has poles at  $\tilde{k}_0 = -m_\varphi \sum_{J=1}^I \varepsilon_J \pm \sqrt{\mathbf{k}_I^2 + \xi_I}$  ( $I = 1 - 2p$ ) and, after  $\tilde{k}_0$ -integration,  $I_{\mathcal{F}}$  becomes

$$\begin{aligned} I_{\mathcal{F}} &= -\pi \lim_{\xi \rightarrow m_\chi^2} \sum_{i=1}^{2p} \int \frac{d^3 \tilde{\mathbf{k}}}{(2\pi)^4} \left[ \frac{1}{2\tilde{k}_0} \prod_{I \neq i} (k_I^2 - \xi_I + i0^+)^{-1} \right]_{\tilde{k}_0 = -m_\varphi \sum_{J=1}^I \varepsilon_J + \sqrt{\mathbf{k}_I^2 + \xi_I}} \\ &= -\pi \lim_{\xi \rightarrow m_\chi^2} \sum_{i=1}^{2p} \int \frac{d^4 \tilde{k}}{(2\pi)^4} \delta(k_i^2 - \xi_i) \prod_{I \neq i} (k_I^2 - \xi_I + i0^+)^{-1}, \end{aligned} \quad (\text{A.4})$$

where, in the second equality, the  $\tilde{k}_0$ -integration is performed in the region where  $k_{i0} \geq 0$ . Using the relation  $(x + i0^+)^{-1} = P(x^{-1}) - i\pi\delta(x)$  (where “ $P$ ” is for the principal value), we obtain

$$\Im[I_{\mathcal{F}}] = 2\pi^2 \lim_{\xi \rightarrow m_\chi^2} \sum_{i=1}^{2p-1} \sum_{j=i+1}^{2p} \int \frac{d^4 \tilde{k}}{(2\pi)^4} \delta(k_i^2 - \xi_i) \delta(k_j^2 - \xi_j) \prod_{I \neq i,j} (k_I^2 - \xi_I)^{-1}. \quad (\text{A.5})$$

Substituting the above expression into Eq. (3.5), we obtain Eq. (3.9).

With the quantity  $N_\varphi = \left| \sum_{I=i+1}^j \varepsilon_I \right|$ ,  $k_i$  and  $k_j$  are related as  $k_i = k_j + N_\varphi Q_\varphi$  (or  $k_i = k_j - N_\varphi Q_\varphi$ ). Thus, if  $N_\varphi = 0$ ,  $k_i = k_j$  and the imaginary part vanishes. Notice also that the constraints from the  $\delta$ -functions can be solved; by shifting the integration variable  $\tilde{k}$ ,  $k_i$  and  $k_j$  can be taken to be  $\tilde{k}$  and  $\tilde{k} - N_\varphi Q_\varphi$ , respectively. Then, the constraints from the  $\delta$ -functions become  $\tilde{k} Q_\varphi = \frac{1}{2} N_\varphi m_\varphi^2$ . Consequently, the product  $\prod_{I \neq i,j} (k_I^2 - \xi_I)^{-1}$  becomes  $\tilde{k}$ -independent. The remaining part is proportional to the two-body phase space for the process where the parent particle with mass  $N_\varphi m_\varphi$  decays into two daughter particles with masses  $\xi_i^{1/2}$  and  $\xi_j^{1/2}$ :

$$\int \frac{d^4 \tilde{k}}{(2\pi)^4} \delta(k_i^2 - \xi_i) \delta(k_j^2 - \xi_j) = \frac{1}{32\pi^3} B(N_\varphi^2 m_\varphi^2; \xi_i, \xi_j), \quad (\text{A.6})$$

where, for  $\sqrt{Q^2} > \xi_i^{1/2} + \xi_j^{1/2}$ ,

$$B(Q^2; \xi_i, \xi_j) \equiv \frac{1}{Q^2} \sqrt{(Q^2)^2 - 2(\xi_i + \xi_j)Q^2 + (\xi_i - \xi_j)^2}, \quad (\text{A.7})$$

while  $B(Q^2; \xi_i, \xi_j) = 0$  for  $\sqrt{Q^2} \leq \xi_i^{1/2} + \xi_j^{1/2}$ . Notice that the function  $B$  is related to  $\beta_{N_\varphi}$  given in Eq. (3.16) as

$$\beta_{N_\varphi} = B(N_\varphi^2 m_\varphi^2; m_\chi^2, m_\chi^2). \quad (\text{A.8})$$

## B Derivation of Eq. (3.21)

In this Appendix, we calculate the imaginary part of the following integral

$$I_{\text{Fig.3}} = -i \int \frac{d^4 \tilde{k}}{(2\pi)^4} (\tilde{k}^2 - m_\chi^2 + i0^+)^{-p} [(\tilde{k} - Q_\varphi)^2 - m_\chi^2 + i0^+]^{-p}, \quad (\text{B.1})$$

to derive Eq. (3.21) from Eq. (3.20). Using the procedure given in Appendix A, we express  $I_{\text{Fig.3}}$  as

$$I_{\text{Fig.3}} = -i \lim_{\xi^{(\prime)} \rightarrow m_\chi^2} \int \frac{d^4 \tilde{k}}{(2\pi)^4} \prod_{I=1}^p (\tilde{k}^2 - \xi_I + i0^+)^{-1} \prod_{J=1}^p [(\tilde{k} - Q_\varphi)^2 - \xi'_J + i0^+]^{-1}. \quad (\text{B.2})$$

The imaginary part of this quantity is obtained with

$$\prod_{I=1}^p (\tilde{k}^2 - \xi_I + i0^+)^{-1} \rightarrow -i\pi \sum_{i=1}^p \prod_{I \neq i} (\xi_i - \xi_I)^{-1} \delta(\tilde{k}^2 - \xi_i), \quad (\text{B.3})$$

and with the similar replacement of the second product. Then, the imaginary part of  $I_{\text{Fig.3}}$  becomes

$$\Im [I_{\text{Fig.3}}] = \frac{1}{16\pi} \lim_{\xi^{(\prime)} \rightarrow m_\chi^2} \sum_{i=1}^p \sum_{j=1}^p \prod_{I \neq i} (\xi_i - \xi_I)^{-1} \prod_{J \neq j} (\xi'_J - \xi'_J)^{-1} B(m_\varphi^2; \xi_i, \xi'_j). \quad (\text{B.4})$$

We can use the relation:

$$\lim_{x_1 \rightarrow x} \cdots \lim_{x_p \rightarrow x} \sum_{i=1}^p f(x_i) \prod_{j \neq i} (x_i - x_j)^{-1} = \frac{1}{(p-1)!} \frac{d^{p-1}}{dx^{p-1}} f(x), \quad (\text{B.5})$$

to obtain

$$\Im [I_{\text{Fig.3}}] = \frac{1}{16\pi} \frac{1}{[(p-1)!]^2} \left[ \frac{\partial^{(p-1)}}{\partial \xi^{(p-1)}} \frac{\partial^{(p-1)}}{\partial \xi'^{(p-1)}} B(m_\varphi^2; \xi, \xi') \right]_{\xi=\xi'=m_\chi^2}. \quad (\text{B.6})$$

Taking the  $O(\beta_1^{1-4(p-1)})$  term from the above expression, which is the most singular one when  $\beta_1 \rightarrow 0$ , Eq. (3.21) is derived.

## References

- [1] A. H. Guth, Phys. Rev. D **23** (1981) 347.
- [2] K. Sato, Mon. Not. Roy. Astron. Soc. **195** (1981) 467.
- [3] A. D. Linde, Phys. Lett. B **108** (1982) 389.

- [4] A. Albrecht and P. J. Steinhardt, Phys. Rev. Lett. **48** (1982) 1220.
- [5] D. N. Spergel *et al.* [WMAP Collaboration], Astrophys. J. Suppl. **170** (2007) 377.
- [6] K. Enqvist and M. S. Sloth, Nucl. Phys. B **626** (2002) 395.
- [7] D. H. Lyth and D. Wands, Phys. Lett. B **524** (2002) 5.
- [8] T. Moroi and T. Takahashi, Phys. Lett. B **522** (2001) 215 [Erratum-ibid. B **539** (2002) 303].
- [9] I. Affleck and M. Dine, Nucl. Phys. B **249** (1985) 361.
- [10] L. Kofman, A. D. Linde and A. A. Starobinsky, Phys. Rev. Lett. **73** (1994) 3195.
- [11] Y. Shtanov, J. H. Traschen and R. H. Brandenberger, Phys. Rev. D **51** (1995) 5438.
- [12] M. Yoshimura, Prog. Theor. Phys. **94** (1995) 873.
- [13] L. Kofman, A. D. Linde and A. A. Starobinsky, Phys. Rev. D **56** (1997) 3258.
- [14] R. P. Feynman and F. L. Vernon, Annals Phys. **24** (1963) 118.
- [15] R. P. Feynman and A. R. Hibbs, *Quantum Mechanics and Path Integral* (McGraw-Hill, New York, 1965).
- [16] S. Matsumoto and M. Yoshimura, Phys. Rev. D **61** (2000) 123509.